

Figure S1. Geographic locations of sampled *D. pseudoobscura* Y chromosomes. See Table S1 for more information.

Wild-type male



Sequenced strain female



Backcross 1 male



Y-replacement strain male (Backcross 9)



Figure S2. Backcrossing scheme to generate Y-replacement lines using wild-type males and the sequenced strain female (backcross strain).

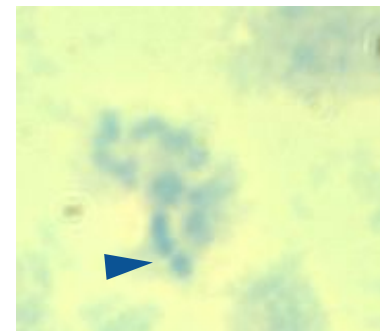
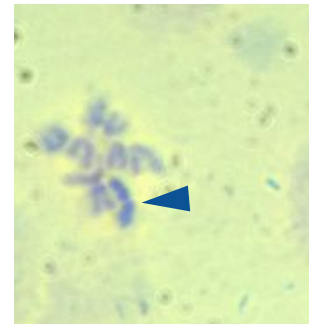
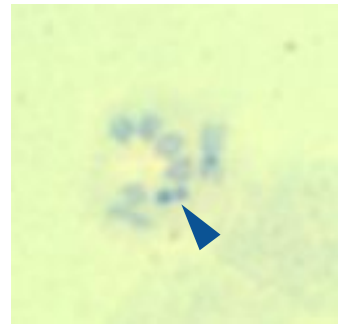
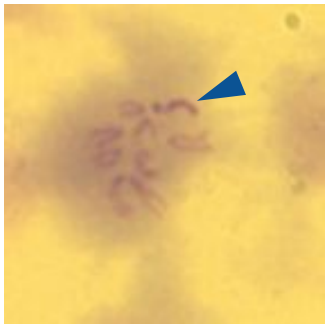


Figure S3. Representative chromosome squashes of Y-replacement line males. Top shows example images of Y chromosome morphology and bottom shows the Y chromosomes with varying sizes.

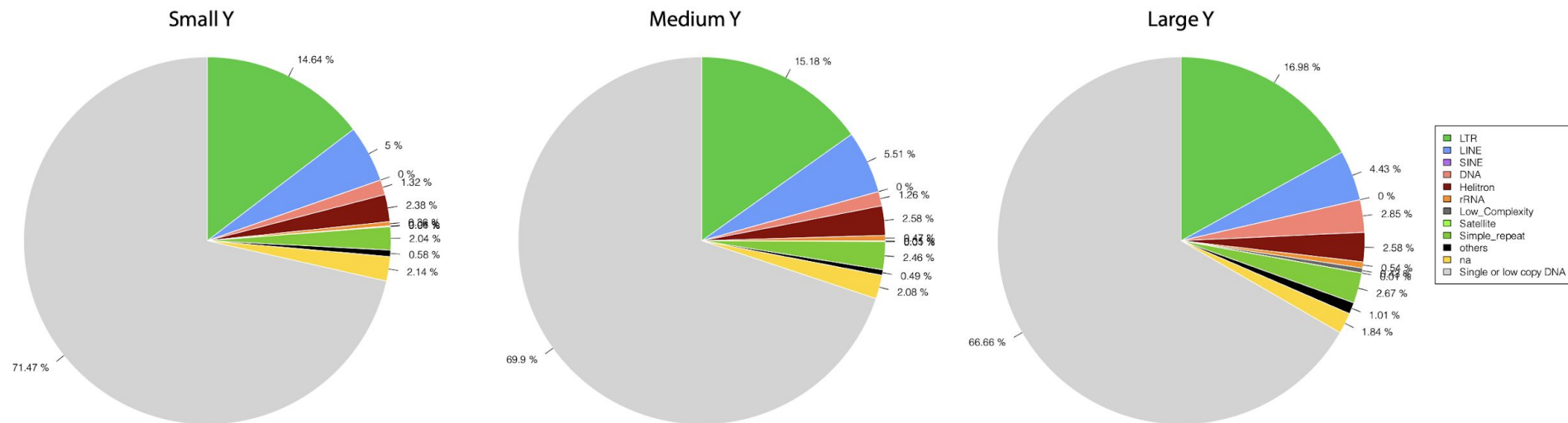


Figure S4. Reference-free based TE and single-copy (euchromatin) estimates for Y_S , Y_M , and Y_L calculated from DNAPipeTE. Grey area denotes % of sample containing single-copy, i.e. euchromatin, DNA with the remaining denoting repetitive content.

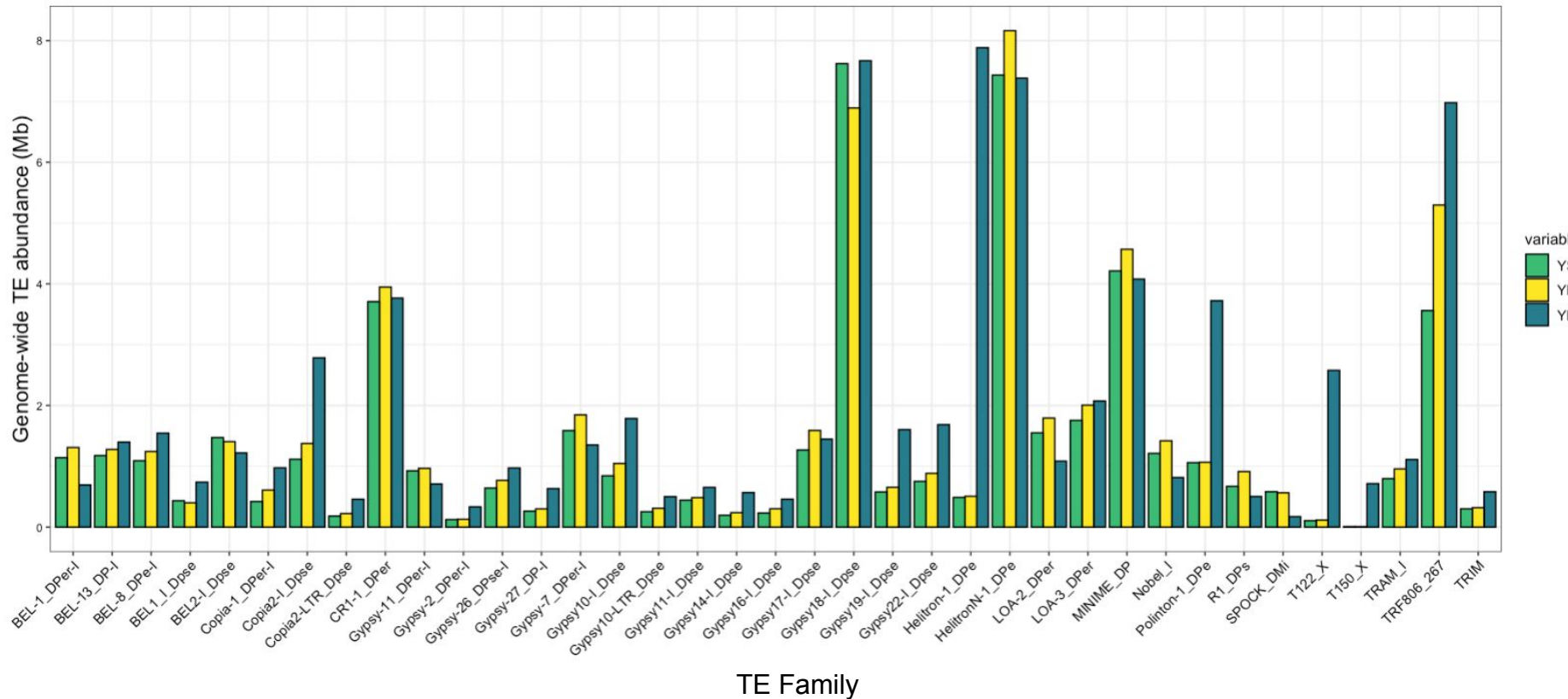
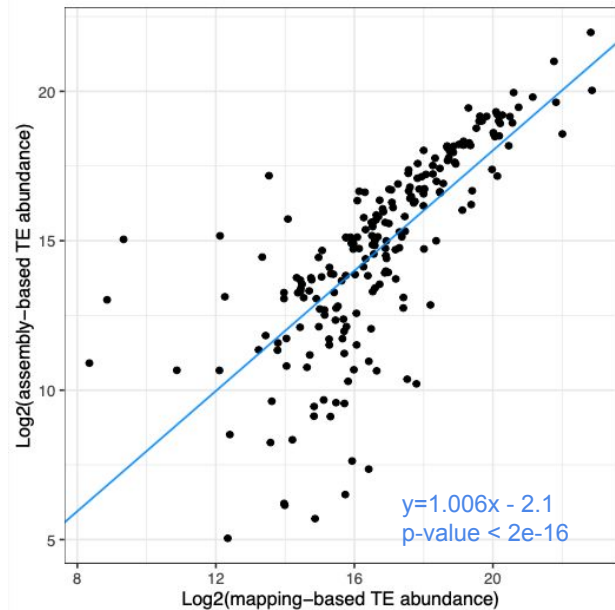
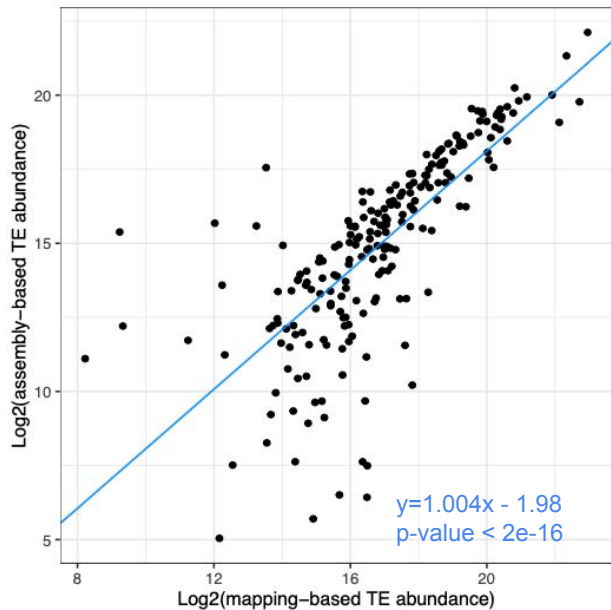


Figure S5. Total TE abundance for Y_S , Y_M , and Y_L males as derived from Illumina mapping. Data underlying figures is contained in Table S11. Note these are absolute amounts compared to relative amounts which are plotted in Figure 3A.

Small Y



Medium Y



Large Y

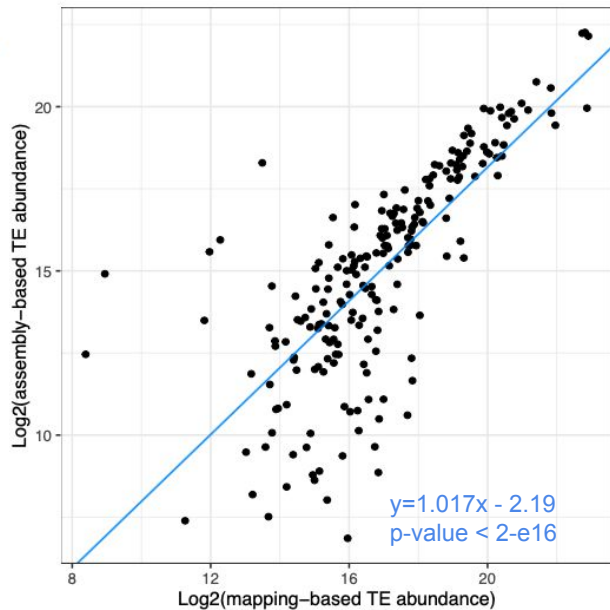
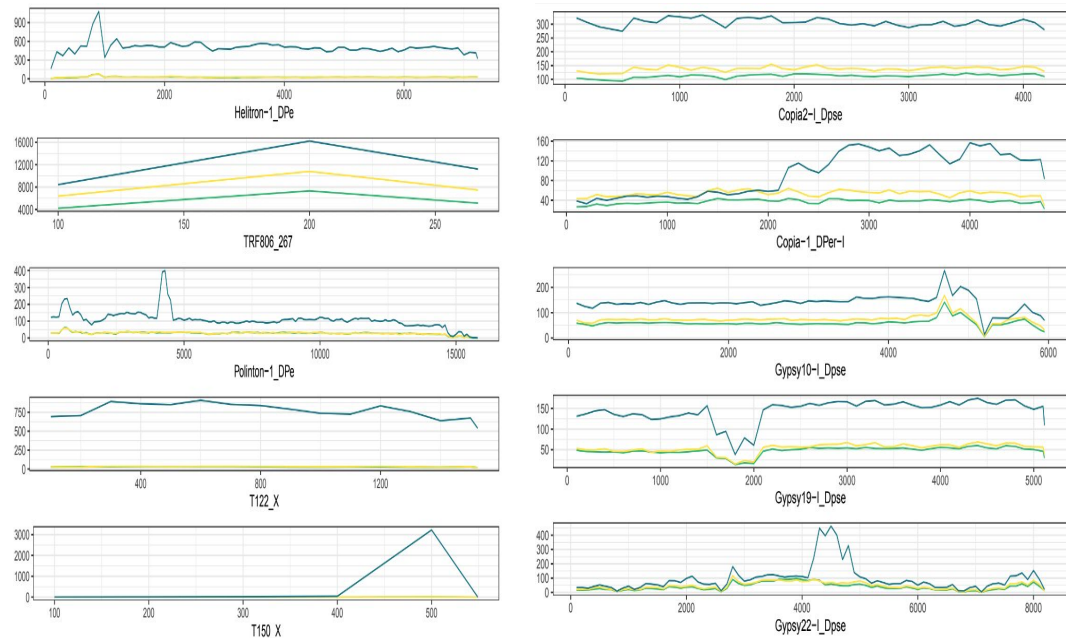


Figure S6. Correlation between Illumina mapping (X-axis) and de novo assembly (Y-axis). TE abundances for Y_S (left), Y_M (middle), and Y_L (right). For each plot, each data point represents a TE family and its respective abundance calculated from Illumina mappings and repeat-masked Y chromosome assemblies. Data underlying these figures are contained in Table S11 and Table S12.

A.



Y_S male
 Y_M male
 Y_L male

B.

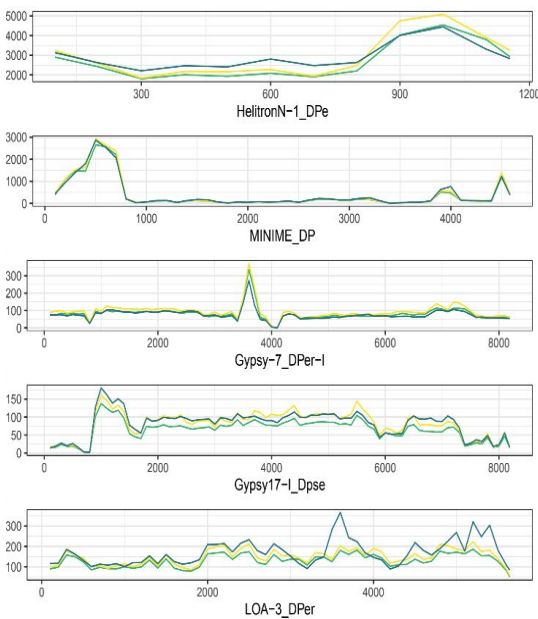
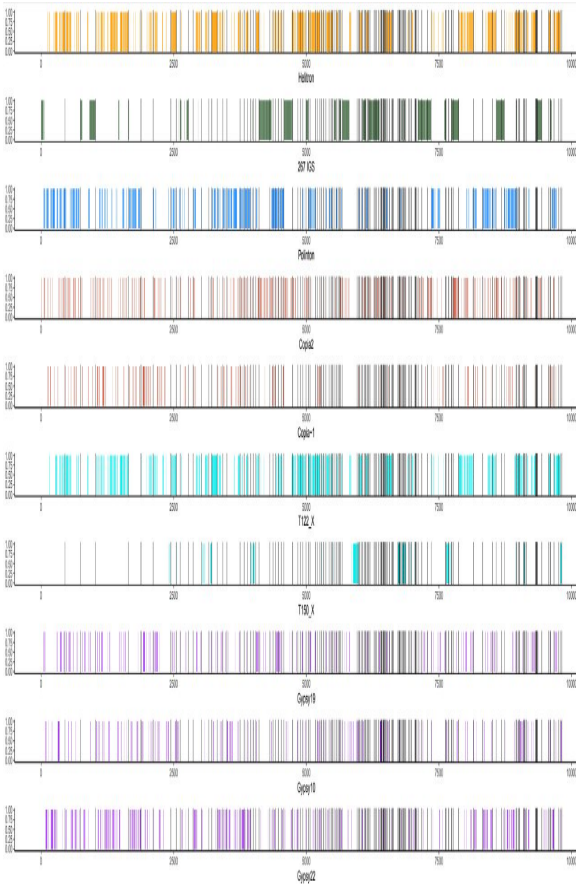
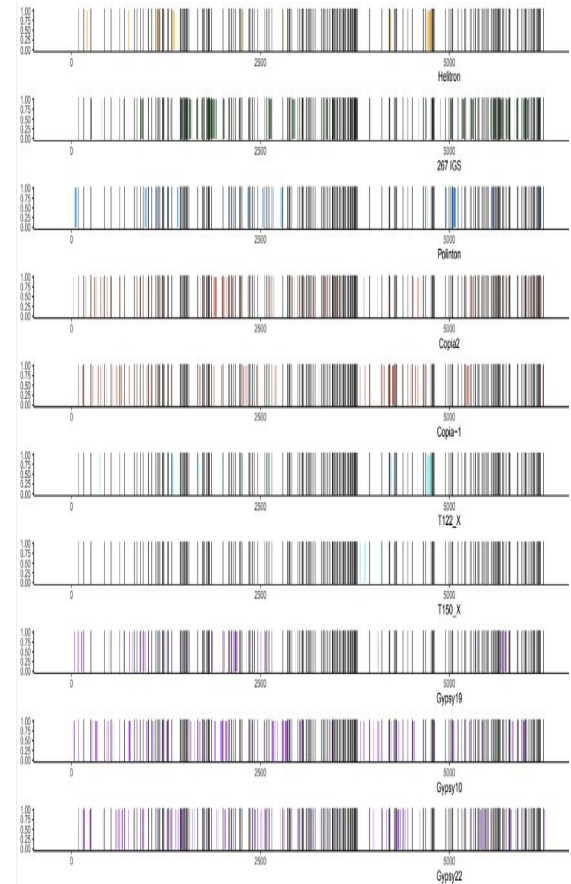


Figure S7. The most abundant transposons in Y_L from Illumina mappings for (A) Y_L and (B) Y_M and their coverage from Y_S , Y_M , and Y_L genomic DNA.

A.



B.



C.

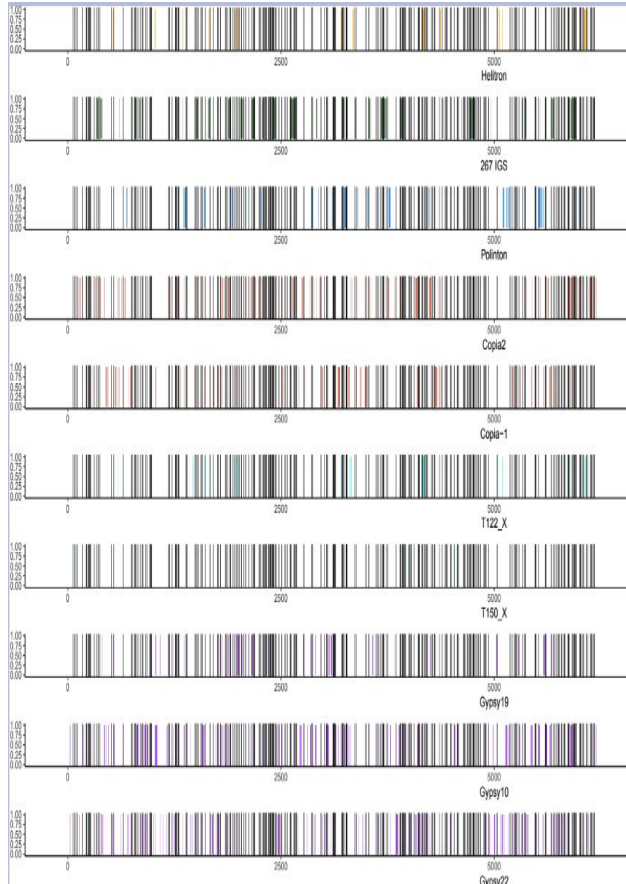


Figure S8 (A-C). TE distribution on Y-linked scaffolds for (A) Y_L , (B) Y_M , and (C) Y_S for the most abundant TEs in Y_L . One X-axis tick corresponds to a 1-5kb window whereas the Y-axis is mainly used for plotting the absence/presence of a TE. Note that assemblies are not adjusted for contig coverage in this figure.

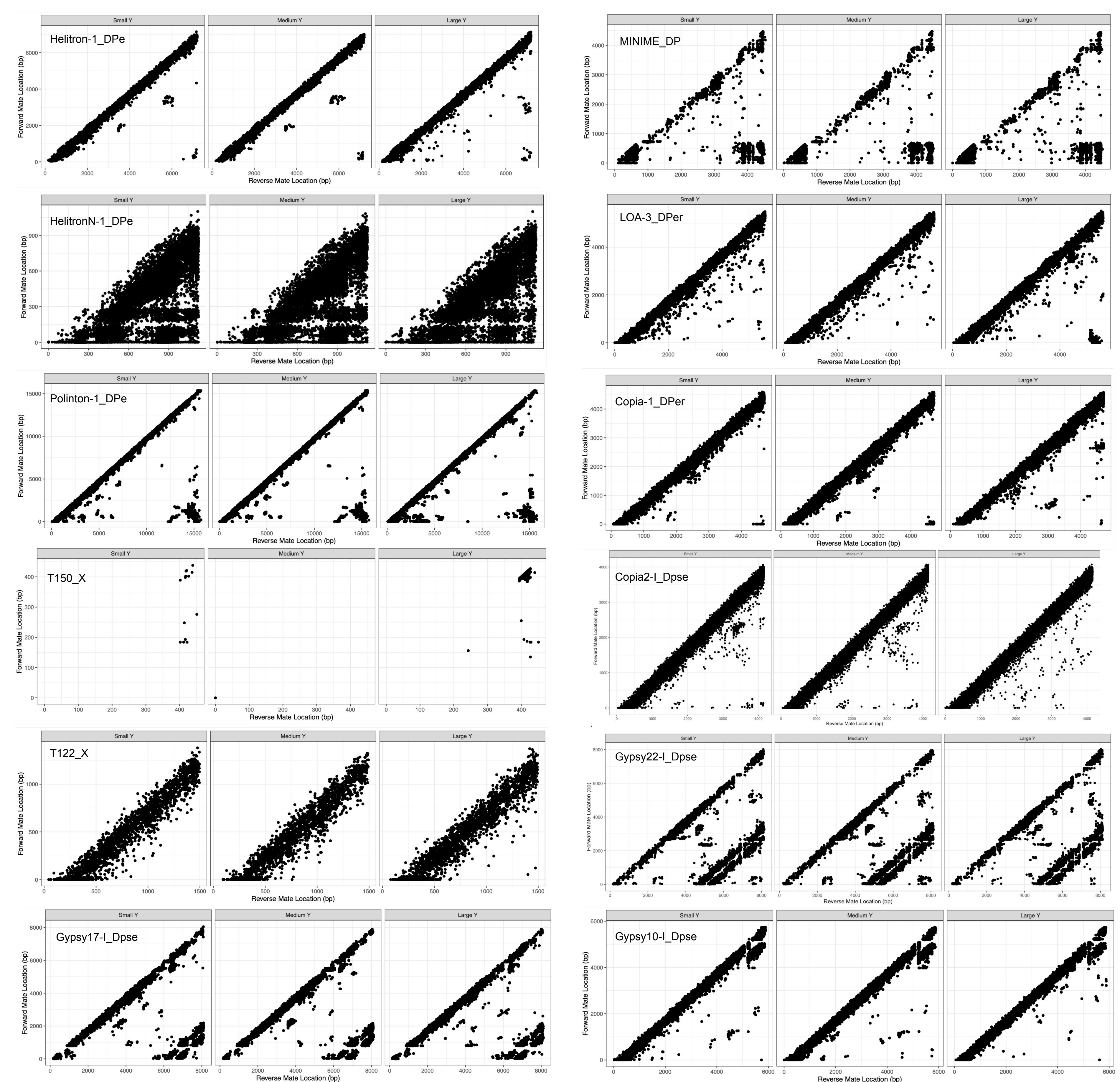


Figure S9. Inferring tandemly repeated TEs using violations of forward and reverse mapping coordinates for a subset of TEs in Y_s , Y_M , and Y_L genomic DNA. Each group of plots corresponds to mapping coordinates of a particular TE for Y_s (left), Y_M (middle), and Y_L (right); the name of the TE is shown in the top-left corner of the Y_s plot. TEs that have head-to-tail tandems will have clusters of reads in the bottom right corner. For each TE, reads are downsampled to the smallest Y chromosome sample with the exception of T150_X where Y_M has no reads.

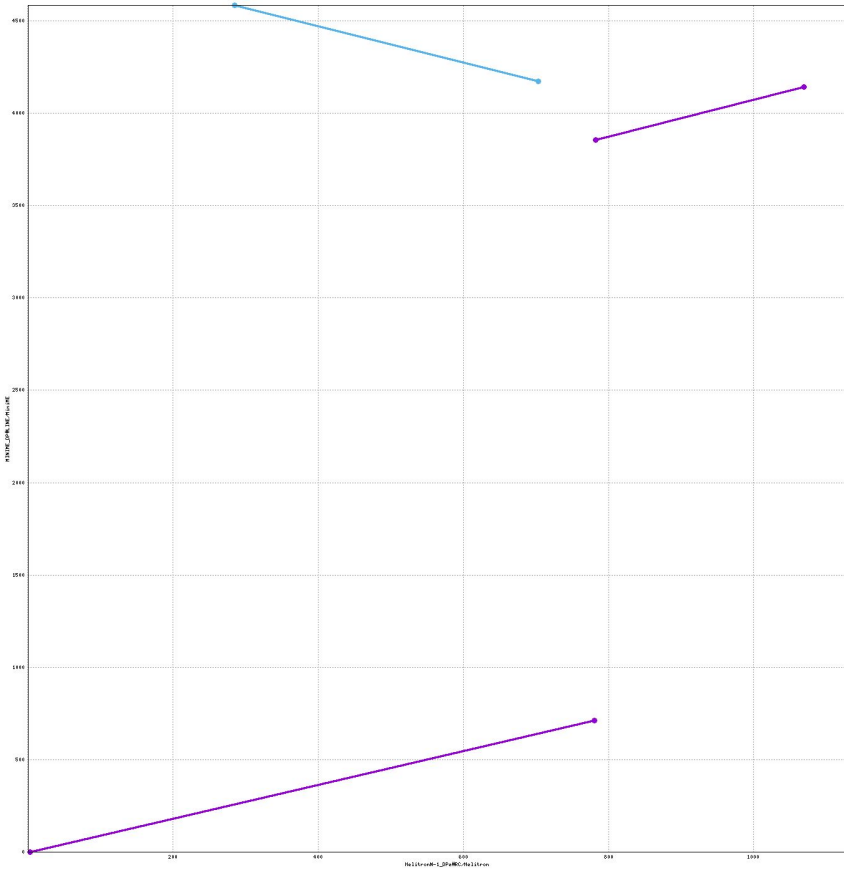


Figure S10. Alignment of HelitronN-1_DPe (X-axis) to MINIME_DP (Y-axis) using nucmer.

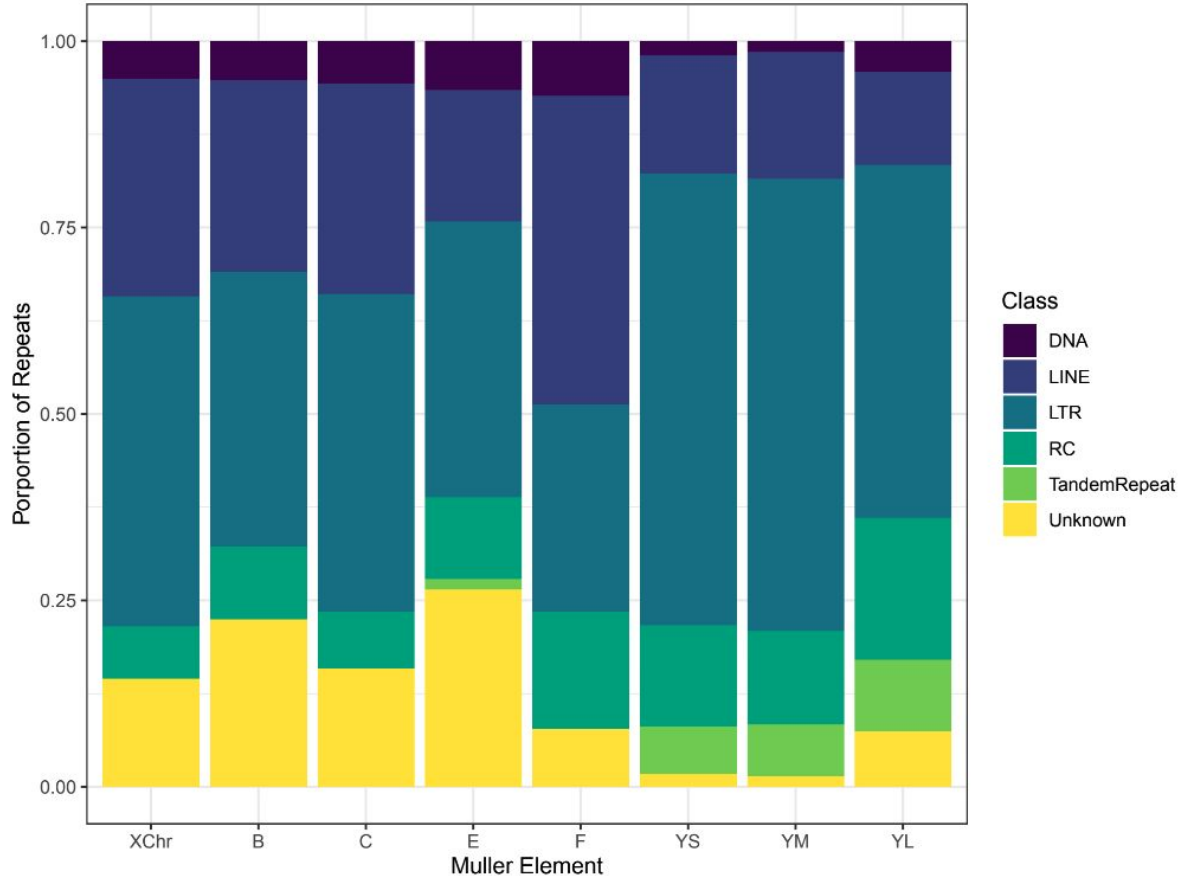


Figure S11. Repeat composition on a per chromosome basis. Shown is the repeat content for the autosomes, X, and the 3 different Y chromosomes from RepeatMasker.

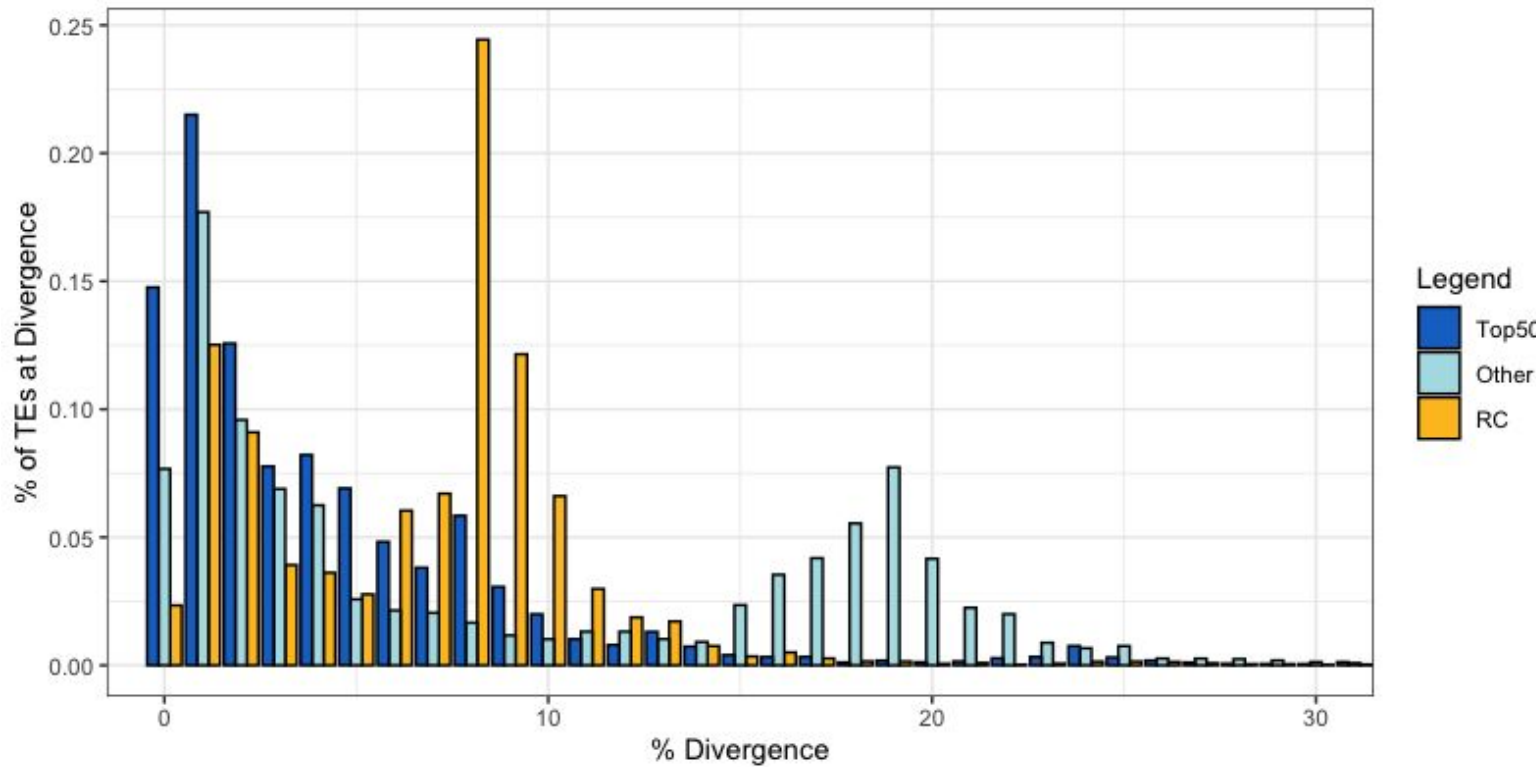


Figure S12. Divergence of abundant/non-abundant TEs on Y_M relative Y_S . The categories are analogous to the ones described in Figure 3D.

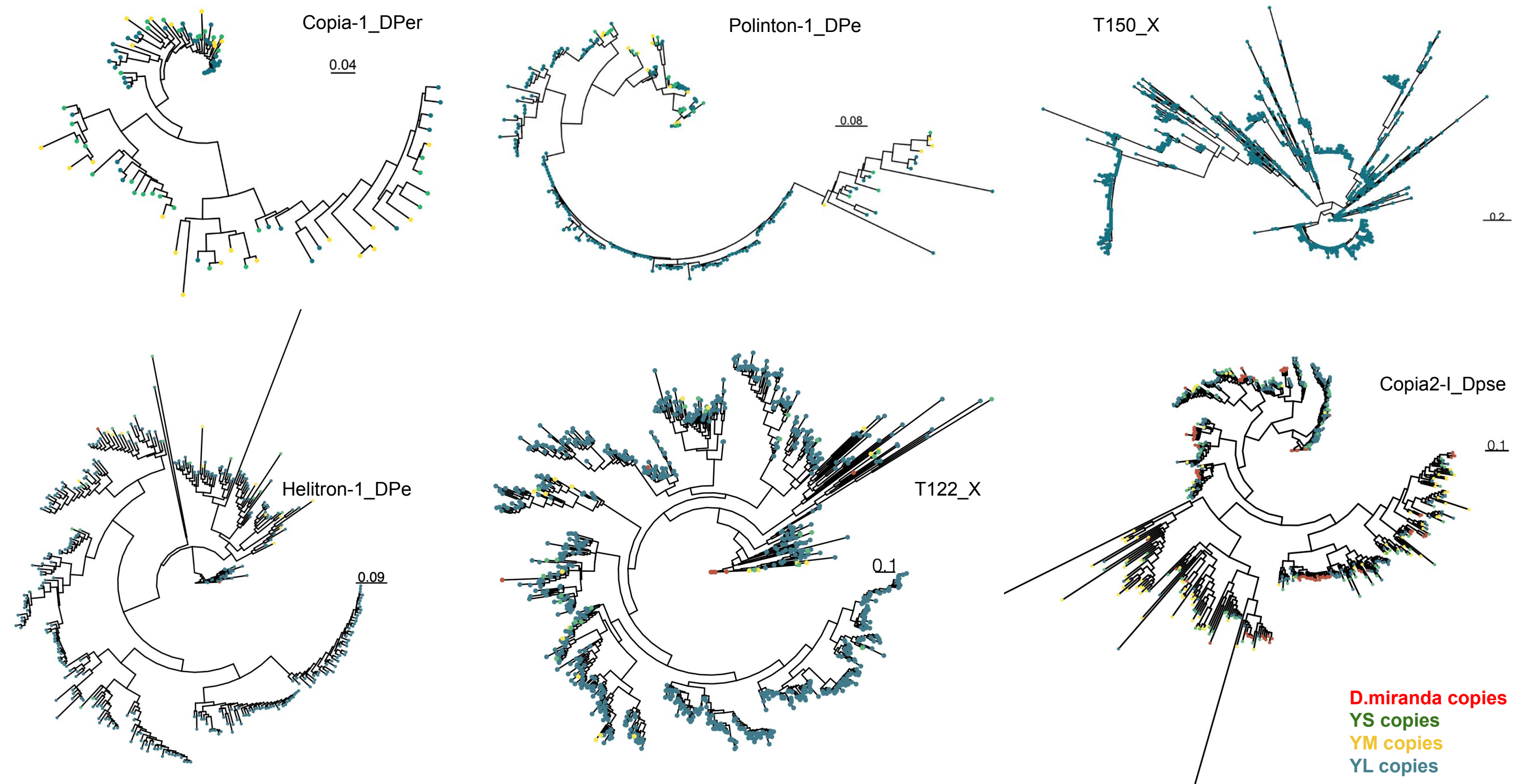


Figure S13. Unrooted phylogenies of TE copies found in Y_S , Y_M , Y_L assemblies. *D. miranda* copies are identified for Copia2-I_Dpse, T122_X, and Helitron-1_DPe.

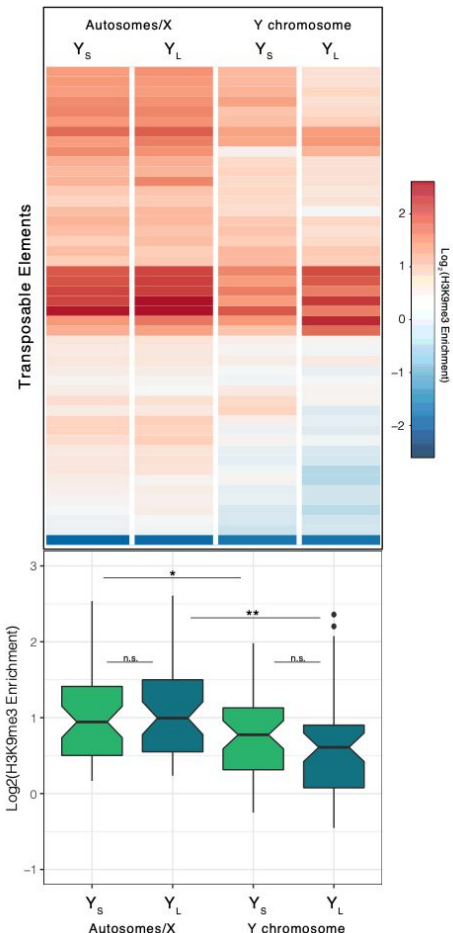


Figure S14. H3K9me3 enrichment for TEs with 50% more copy number in either Y_s or Y_L . Top shows enrichment plotted in heatmap with each row corresponding to a TE and bottom shows the same data in boxplot form.

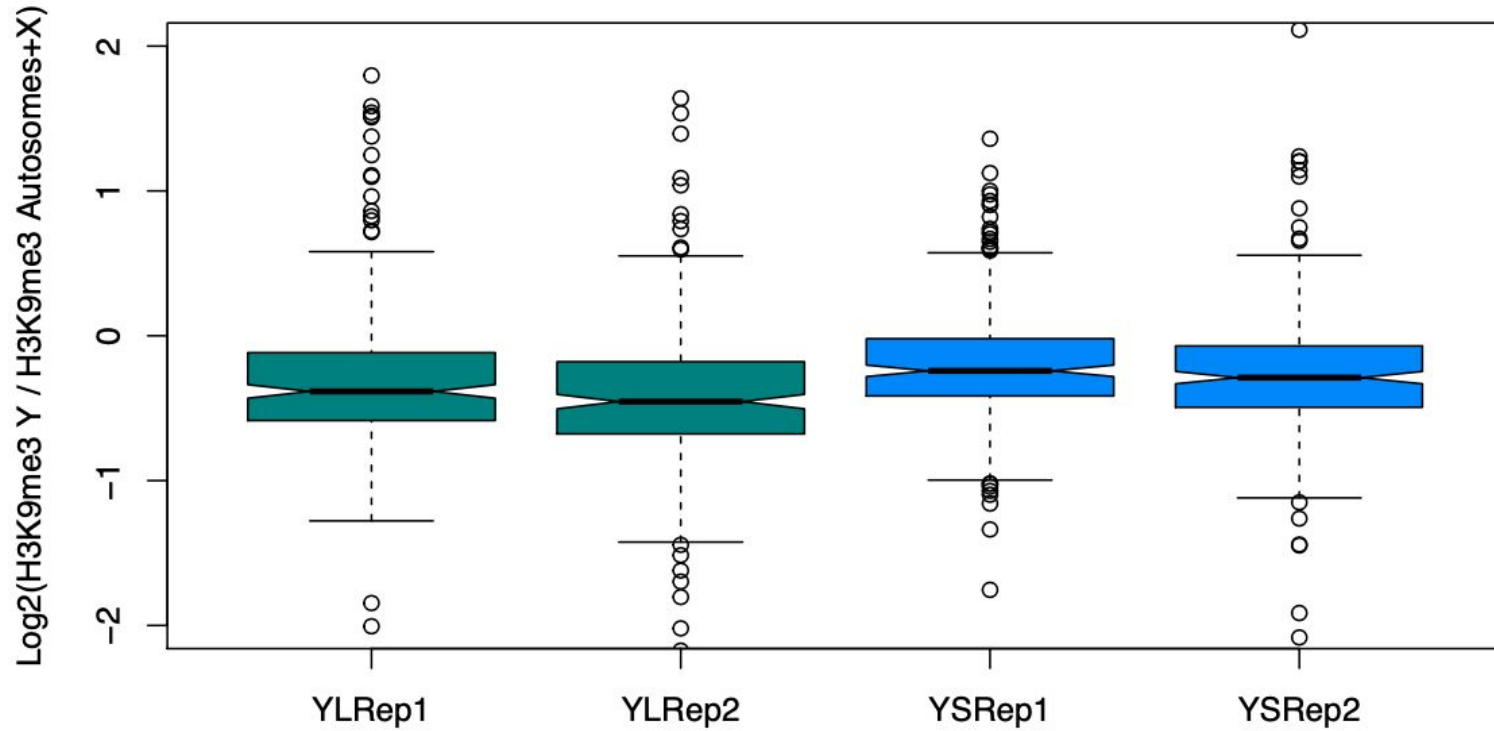


Figure S15. $\text{Log2}(\text{H3K9me3 } T_E_Y / \text{H3K9me3 } T_E_{\text{Auto}/X})$ for all Y_s and Y_l ChIP replicates shown as boxplots.

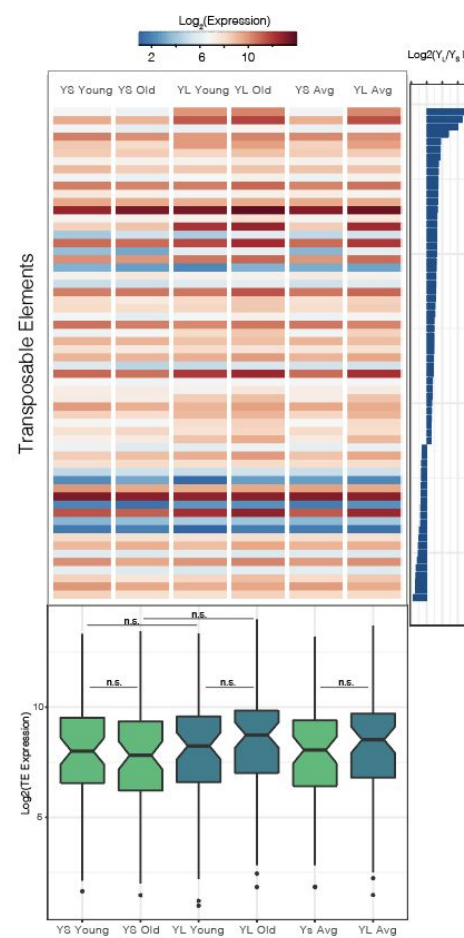
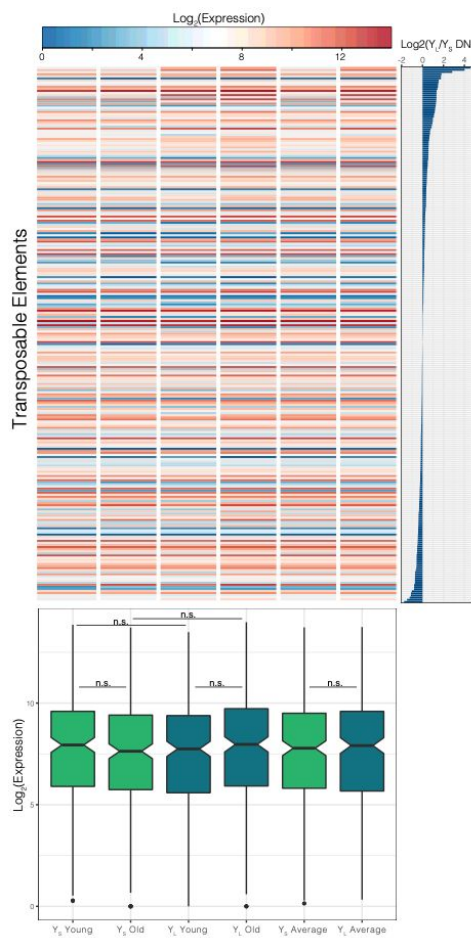
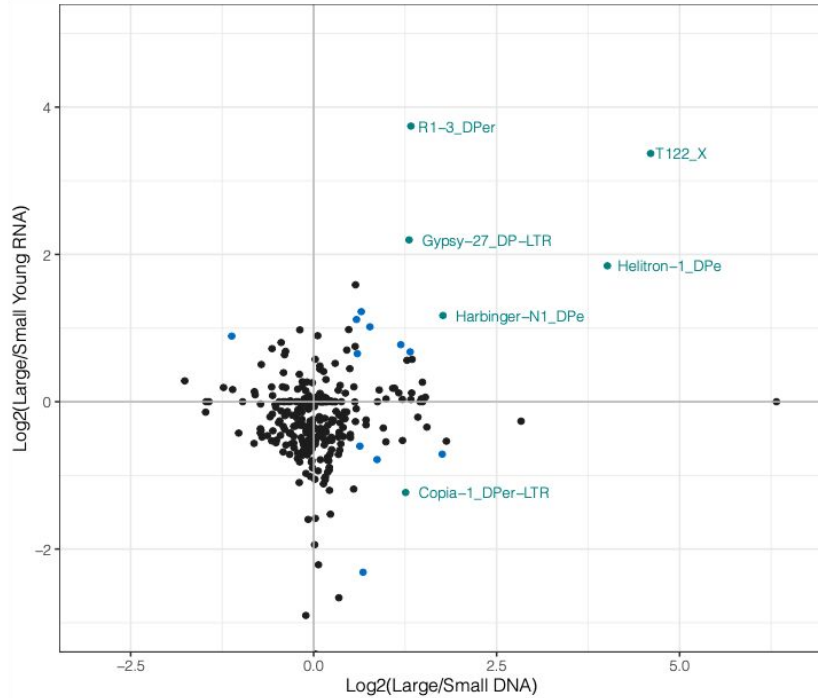


Figure S16. TE expression by Y-replacement line and age, sorted by TE abundance. (A) All TEs with $\text{Log2(expression)} > 1$. (B) All TEs with $\text{Log2(expression)} > 1$ and 50% more TE abundance in either Y_s or Y_l .

Young samples



Old samples

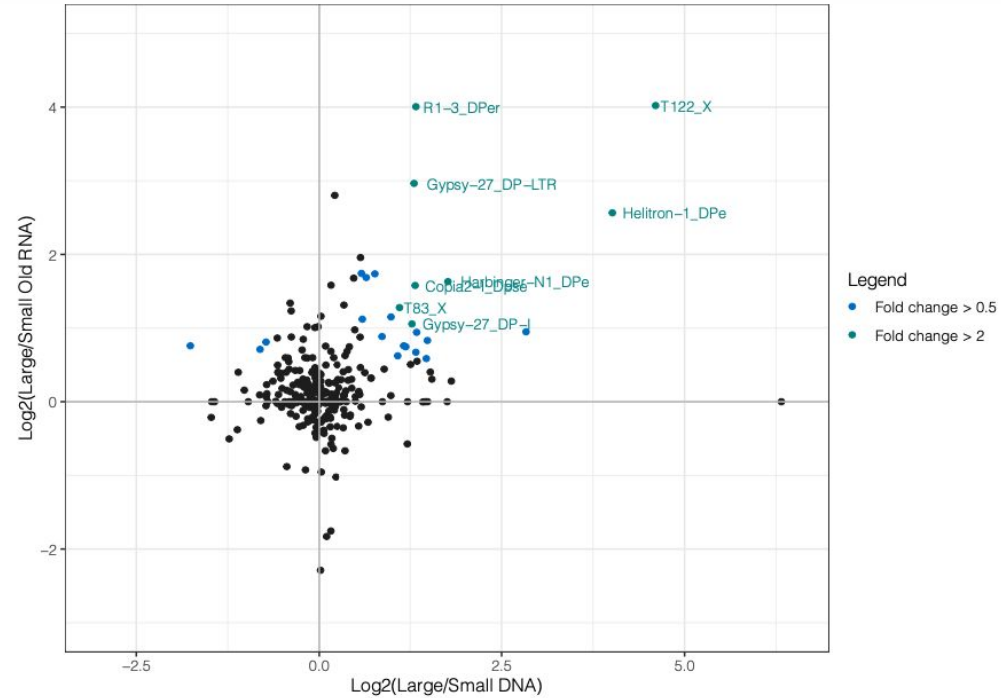
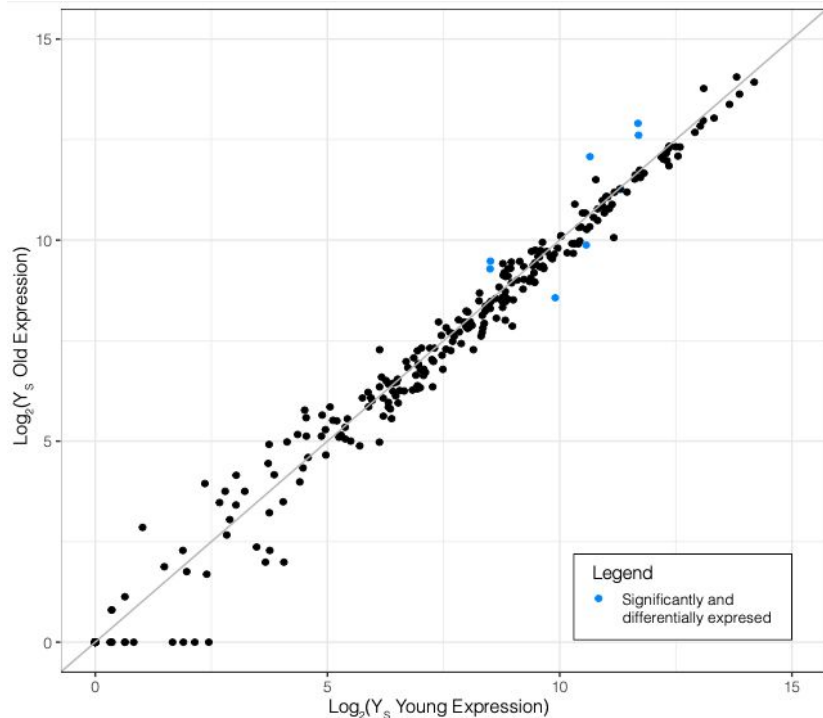


Figure S17. TE abundance differences vs TE expression differences in Y-replacement line males by age (left: young, right: old). Each data point represents a TE with its associated difference in abundance/expression between Y_s and Y_L . Plots were made from the same data that underlies Figure 4C.

Small Y-replacement line males



Large Y-replacement line males

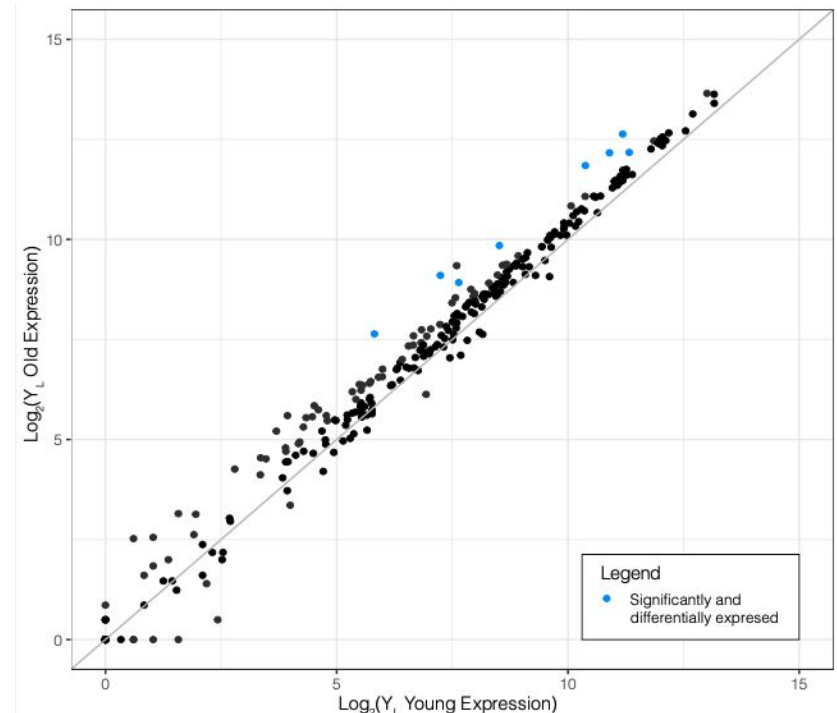


Figure S18. Age-associated TE expression differences within Y-replacement line males. Left: Y_s males, right: Y_l males. Blue data indicates at least 50% significant differential expression (Wald-test, p -value < 0.05).

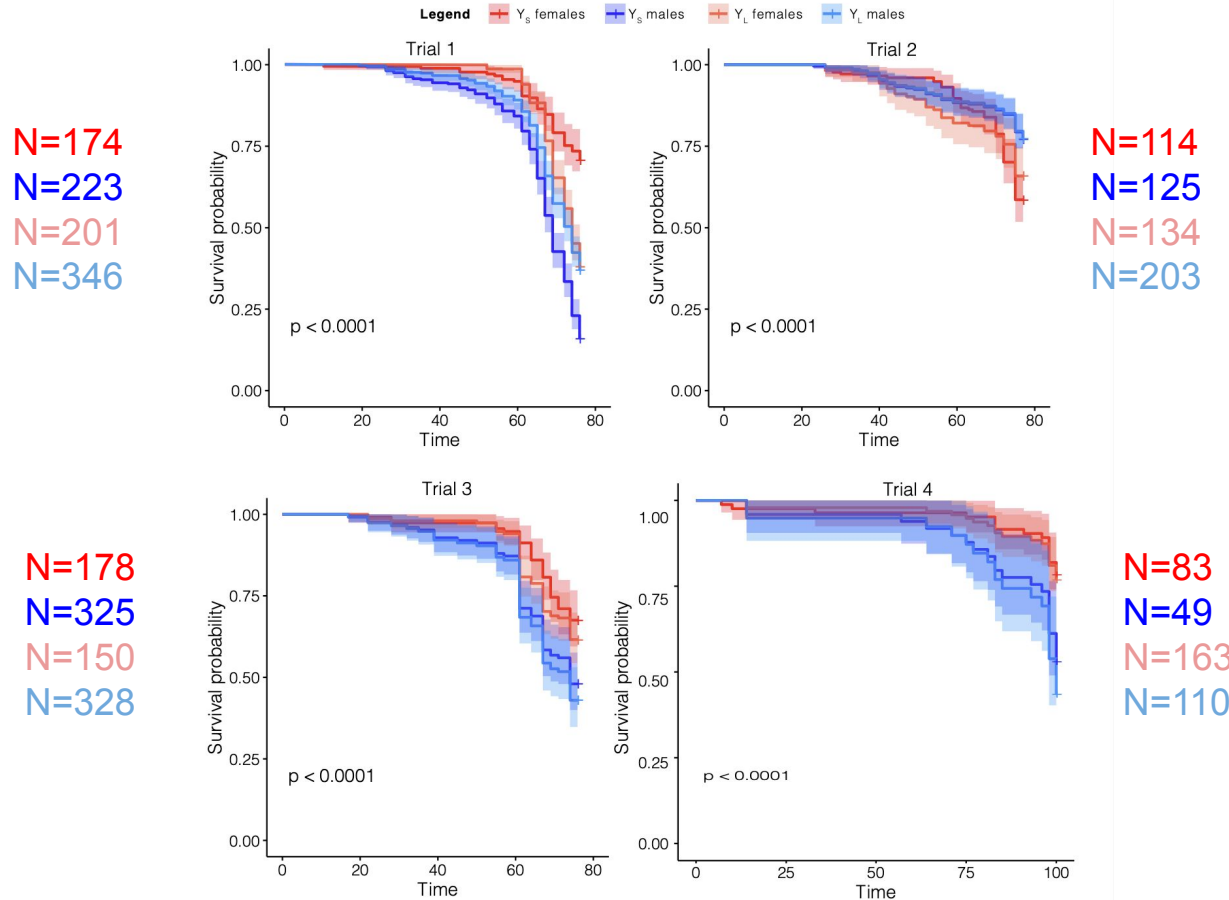


Figure S19. Y-replacement line aging trials recorded separately. All aging trials are shown with females from both Y-replacement line males plotted as individual tracks.

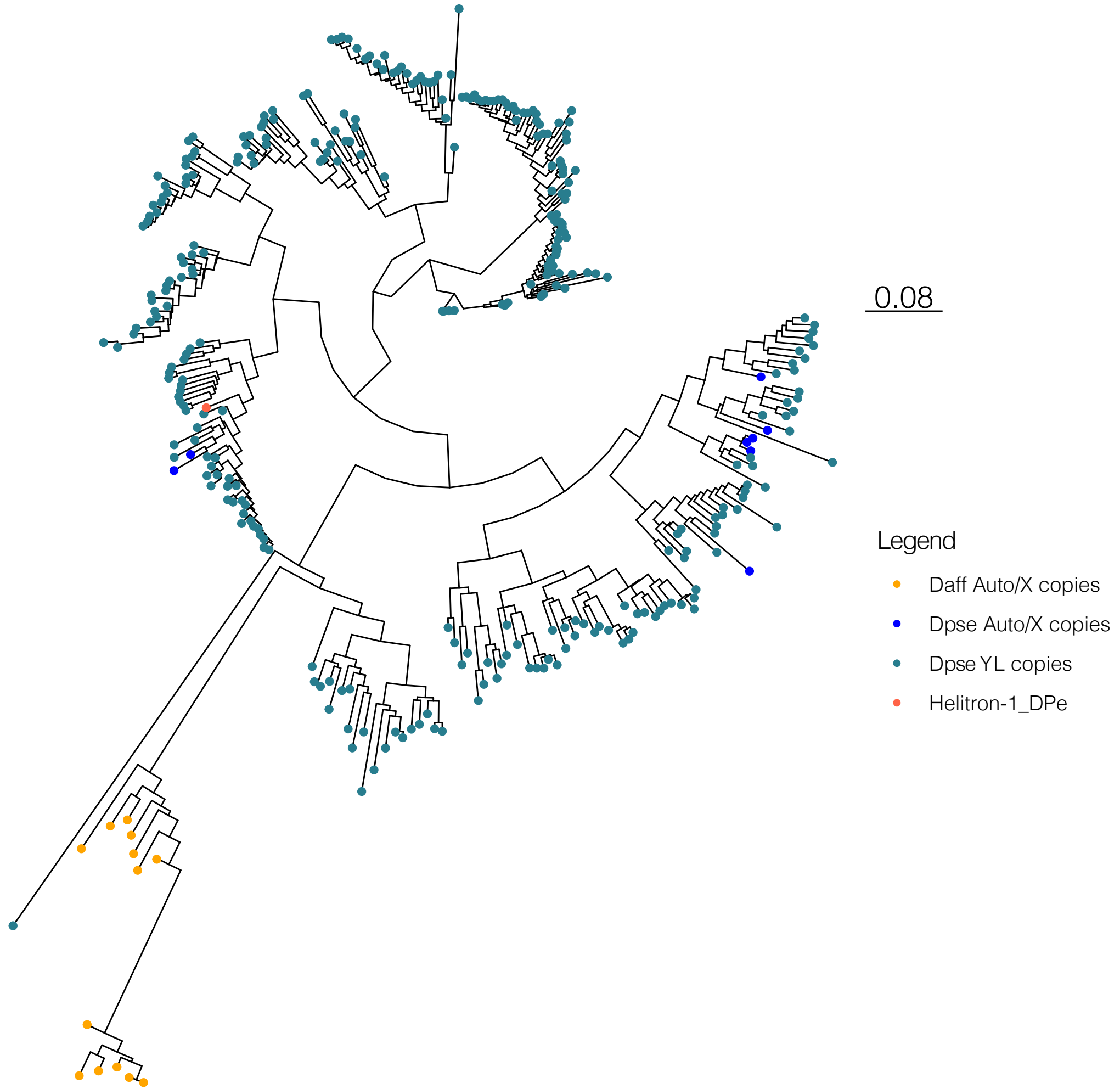


Figure S20. Phylogeny of Helitron elements from the *D. pseudoobscura* autosomes/X, *D. pseudoobscura* YL, and *D. affinis* autosomes/X.